

Gold nanoparticle layers from multi-step adsorption immobilised on a polymer surface during injection molding

Felix Kroschwald,¹ Jürgen Nagel,¹ Andreas Janke,¹ Frank Simon,¹ Cordelia Zimmerer,¹ Gert Heinrich,^{1,2} Brigitte Voit^{1,3}

¹Leibniz-Institut für Polymerforschung Dresden e.V, Hohe Straße 6, Dresden 01069, Germany

²Institut für Werkstoffwissenschaft, Technische Universität Dresden, Hohe Straße 6, Dresden 01069, Germany

³Department Chemistry and Food Chemistry, Organic Chemistry of Polymers, Technische Universität Dresden, Hohe Straße 6, Dresden 01069, Germany

Correspondence to: J. Nagel (E-mail: nagel@ipfdd.de)

ABSTRACT: Functional nanoparticles exhibit, e.g., a chemical functionality. For their use, a reliable immobilisation is often required. Here, a method is described, how those nanoparticles can be immobilised on a thermoplastic surface using melt processing. Gold nanoparticles (AuNP) are assembled in a layer on a substrate by adsorption. The degree of coverage can be controlled by repeating the adsorption process. During each adsorption step, the particles were arranged on the surface as chain-like aggregates with close particle–particle contacts, rather than as isolated particles. The degree of area coverage on the substrate surface was up to 70%. The AuNP layers were transferred onto the surfaces of polycarbonate (PC) sheets by injection molding. The AuNP were partly embedded by the thermoplastic polymer and in this way permanently immobilised on the part surface. The reduction of methyl orange demonstrated the accessibility of the gold surface for small molecules. Furthermore, the fabrication of bactericide surfaces, sensor surfaces, all using AuNP immobilised on a thermoplastic part surface may become possible. © 2016 Wiley Periodicals, Inc. *J. Appl. Polym. Sci.* **2016**, *133*, 43608.

KEYWORDS: adsorption; molding; monolayers and polymer brushes; nanoparticles; nanowires and nanocrystals; surfaces and interfaces

Received 19 November 2015; accepted 8 March 2016

DOI: 10.1002/app.43608

INTRODUCTION

The catalytic activity of gold was investigated extensively.^{1–4} Gold exhibits catalytic activity for a broad diversity of reactions, e.g., hydrogenations, reactions involving carbon monoxide, oxidations and reductions, and addition reactions.^{5,6} Only recently, gold catalysts are investigated for the photo-catalytic cleavage of water. The catalytic reduction of methyl orange (MO) by BH is often used as model reaction. Hereby, BH donates an electron to gold, whereas gold donates an electron to MO, which reduces MO to a colourless compound. Therefore, the catalytic activity can be simply recorded spectrophotometrically.⁷

Obviously, the catalytic centres are always located on the gold surface, and the activity increases with the surface area. Compared to a thin film of gold, an colloidal solution of gold particles of the size equal to the thickness of the layer exhibits a six times higher surface area. This is reduced by the substrate–particle surface area, if the particles are assembled on a surface. In reality, the surface area is even higher by preparation of rough

surfaces. Therefore, small particles or even gold nanoparticles (AuNP) are often used. However, nanoparticles have to be immobilized on a substrate surface for effective use. Therefore, the immobilisation of nanoparticles on surfaces is an essential issue and a prerequisite for most applications. The nanoparticles are often assembled in a layer on a surface of a material.^{8–10}

For successful adsorption, the compatibility and electrostatic attraction between AuNP and the adsorbent is important. Especially polyethylene imine (PEI) is often used for stabilisation or adsorption of AuNP.^{11–13} Thereby, amino groups stabilise the particles under formation of coordinative bonds.^{14,15} Defined AuNP-PEI layers can be formed by step-by-step electrostatic deposition from aqueous solutions.^{8,9,16} Since most solids have a negative surface charge in water, a polycation is adsorbed in the first step. AuNP then adsorb on this cationic modified surface under formation of a more or less dense monolayer. On repeating of these steps, multilayers are formed. An approach was presented, that enables the AuNP to immobilise on the surface of a polymer melt whereby the particles were covered

Additional Supporting Information may be found in the online version of this article.

© 2016 Wiley Periodicals, Inc.

completely by a thin polymer layer.¹⁷ A recently investigated approach is based on the formation of AuNP layers on a substrate and the transfer of this layer onto the polymer melt during molding.¹⁸ It may become the base for a technical process of manufacturing of polymer parts for special applications, including catalysis, microfluidics, sensing, micro and nanoelectronics, bactericide as well as scratch-resistant surfaces. However, the interactions between the particles on a substrate surface and the polymer melt flowing along the layer surface are not quite understood. An interesting question is, whether and how structures of the AuNP layer on the substrate can be reproduced on deposition to the flowing polymer melt. A second question was, whether the particles are covered completely or only partly by melt and still exhibit a free area accessible for small molecules from solution.

The paper presents results on the preparation of AuNP layers on a substrate surface by adsorption from solution and their deposition to a surface of a thermoplastic part by molding. First, a polycation was adsorbed on the substrate surface to change the surface charge positive. Then, AuNP were adsorbed on this surface. Finally, the substrate was mounted in the mold of an injection molding machine, and a thermoplastic melt was injected. After solidifying, the substrate was removed. The formation of layers on the substrate is investigated in detail. The degree of coverage of AuNP on the substrate surface was increased by use of multiple adsorption steps, whereby the AuNP adsorbed as a pearl necklace rather than as single particles. The layers on the substrate and on the part surface were characterised by optical spectroscopy, atomic force microscopy (AFM) and electron microscopy. Conclusions are made about the transfer process of this new type of deposition approach with emphasis on the processes proceeding in the nanometre region of a flowing melt during the molding process. Finally, the catalytic activity of AuNP embedded in the thermoplastic part surface is investigated. It is compared with that of a AuNP layer on a substrate to assess the transfer process. The results show that the AuNP transferred by injection molding are embedded on the surface layer under widely retaining their structure, and they are still accessible for small molecules.

EXPERIMENTAL

Materials

Tetrachloroauric acid ($\text{HAuCl}_4 \cdot 3\text{H}_2\text{O}$), sodium citrate, sodium chloride, PEI ($M_w = 750.000 \text{ g}\cdot\text{mol}^{-1}$, 50 wt % in aqueous solution), were purchased from Sigma-Aldrich Chemie GmbH, Germany, and used as received. Hydrochloric acid (conc.) was purchased from Merck KGaA, Germany. Solutions were diluted with Milli-Q water having a resistivity less than $0.055 \mu\text{S cm}^{-1}$. The polycarbonate (PC) type Makrolon LED 2025 provided by Bayer Material Science AG, Germany was employed for thermoplastic injection molding experiments.

Methods

Preparation of Solutions. PEI solution was prepared by mixing of 0.2328 mol PEI with 1 mol NaCl. The mixture was filled up to 1 l . The pH value was adjusted to 8 with hydrochloric acid. The colloidal gold solution was prepared following the method of Turkevitch and Frens by adding 1 mL of a $0.025 \text{ mol}\cdot\text{L}^{-1}$

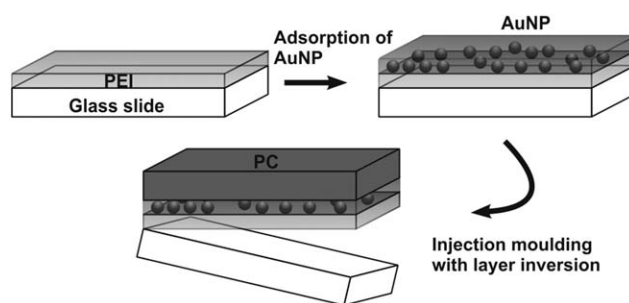


Figure 1. Schematic of the sample preparation for the immobilisation of AuNP on a thermoplastic surface.

aqueous HAuCl_4 solution in water to 100 mL water in a 250 mL two-necked flask. The mixture was heated to 100°C under vigorous stirring.^{19,20} Then 2 mL of a 0.039 mol L^{-1} aqueous sodium citrate solution were added. The mixture was stirred for 15 min . The colloidal solution formed was cooled to room temperature prior to use.

Formation of AuNP Layers on Substrates. Glass slides and mirror-polished steel plates were used as substrates for layer formation. The glass slides were cleaned in NoChromix (75 mL sulphuric acid, 25 mL water, $0.5 \text{ g K}_2\text{S}_2\text{O}_8$) solution for 4 hours and rinsed intensively with water. The steel substrates were used for injection molding experiments. They were cleaned with detergent and rinsed thoroughly with water prior to use.

The clean substrates were immersed for 15 min in PEI solution and then rinsed with water for 15 min . They were then immersed for 60 min in the AuNP solution under formation of a monolayer (samples of type 1X). To remove any loosely adsorbed excess, they were rinsed with water. Repeating the procedure two or three times resulted in the formation of samples of type 2X and 3X, respectively.

Transfer on Polycarbonate Parts during Molding. A BOY 22 A HV (Dr. Boy GmbH & Co. KG, Germany) injection molding machine with a clamping force of 220 kN , and a screw diameter of 18 mm was used for molding investigations. Melt and mold temperatures were 300°C and 80°C , respectively. A special mold with magnetic holder for steel plates as substrates was build in-house. The cavity had a diameter of 20 mm and a sprue located in the centre. The substrates coated with the AuNP layers, see Figure 1, were mounted in the cavity of the mold. Then the melt was injected. The parts were ejected after solidification. They had a thickness of 2.5 mm .

Characterisation of Layers. UV/Vis spectra were recorded using a Lambda 800 spectrometer (Perkin-Elmer Inc., USA). Transmission electron microscopy (TEM) was carried out with a Libra 200 MC (Carl Zeiss AG, Germany). The lamellae were cut with a focused ion beam device (Neon 40 EsB Crossbeam, Carl Zeiss AG, Germany). Atomic force microscopy (AFM) investigations were made with a NanoScope V Dimension 3100 (Bruker Corp., USA). For scanning electron microscopy an Ultra Plus microscope (Carl Zeiss AG, Germany) was used. XPS investigations were performed with an Axis Ultra spectrometer (Kratos Analytical Ltd, UK). Electrokinetic measurements on plane substrates were carried out with an EKA device (Anton Paar

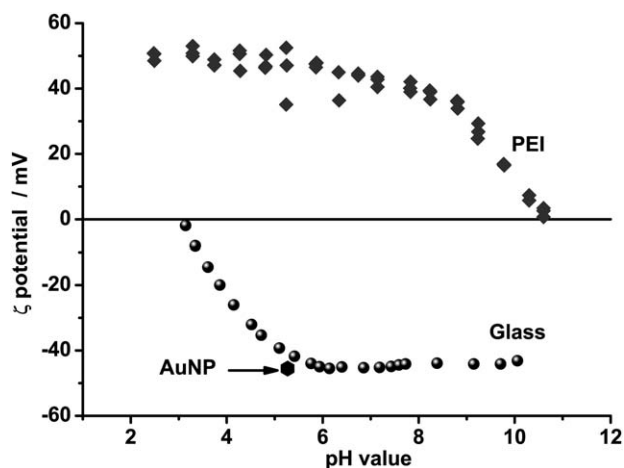


Figure 2. Dependence of the ζ potential on pH values in aqueous KCl solution ($[KCl] = 3 \cdot 10^{-3} \text{ mol L}^{-1}$). The functions $\zeta = \zeta(\text{pH})$ were recorded for a bare glass slide and an aqueous PEI solution. The ζ potential of AuNP was only determined at $\text{pH} = 5.6$ due to the limited stability of the AuNP solution at other pH values.

GmbH, Austria). Particle size distributions and ζ potentials were measured by dynamic light scattering using a Zetasizer Nano ZS (Malvern Instruments Ltd., UK). The ζ potentials of plates (substrates or PC parts) was measured using an EKA Analyser (Anton Paar GmbH, Austria), operated a special sample holder and with a maximum pressure of 250 mbar.

Test of Chemical Activity. Catalysis experiments were carried out in standard glass cuvettes with an optical path length of 10 mm. The cuvette was filled with a solution of 150 μL of MO (0.25 mM) and 1600 μL water. Samples (blind, substrate, PC plate) with appropriate size were mounted on both blind sides of the cuvette, according to a protocol given in the literature.²¹ 150 μL of 80 mM NaBH_4 solution in water were added and the measurements were started. The measurement beam was partly perturbed by bubbles of hydrogen created by the decomposition of the borohydride.

RESULTS AND DISCUSSION

Characterisations of AuNP and of PEI Solution

AuNP were synthesised using the Turkevitch and Frens method, where sodium citrate was used for reduction and stabilisation of the AuNP formed. The mean diameter of the AuNP prepared was about 20 nm according to DLS measurements. The inflection points of the distribution curve were at 10 and 40 nm (see Supporting Information Figure S1). The optical spectrum of the AuNP solution had a maximum absorption wavelength of 521 nm and a marginal higher absorbance at 600 nm. As known from plasmon absorption models, single particles with this size absorb light of a wavelength of about 520 nm, dependent on the dielectric permittivity of the environment.^{22,23} Particle aggregates, on the other hand, absorb at wavelengths above 600 nm.²⁴ Thus, the observed particle absorption characteristics point to mainly single particles in solution.

The ζ potential of AuNP, dispersed in aqueous solution, was -40 mV at $\text{pH} = 5.6$, see Figure 2. Changes of the pH value of

Table I. Sample Preparation and Notation

Starting substrate	Adsorption of	Resulting sample identifier
Glass slide	1.PEI, 2.AuNP	Type 1X
Type 1X	1.PEI, 2.AuNP	Type 2X
Type 2X	1.PEI, 2.AuNP	Type 3X

the AuNP solution resulted in agglomeration and precipitation of the AuNP. Hence, the pH value of the AuNP solution was kept constant. PEI had positive ζ potentials in solution between pH 3 and 10.7. To support an electrostatic adsorption process in aqueous solution, PEI was selected as an appropriate polymer providing a positive ζ potential and a high density of amino groups.

Formation of AuNP-PEI Layers on Substrates

Glass slides were used as substrates for optical and microscopy investigations. Glass surfaces are characterised by a high density of silanol (Si-OH) groups. The dependence of the ζ potential on pH of glass slides used is shown in Figure 2. The isoelectric point (pH value where $\zeta = 0$) was 3.1. The ζ potential decreased up to a pH value of about 6, as a result of the dissociation of the silanol groups. It stayed constant with a value of about -40 mV in the region from pH 6 to the end of the measured interval at pH 10.3. Contrary, the ζ potential of PEI was positive at low pH. It was about $+40 \text{ mV}$ at pH 8. Therefore, adsorptions of PEI from aqueous solution onto glass surfaces were made at pH 8. Adsorptions of AuNP were carried out at pH 5.6.

Samples of type 1X were prepared by immersing a substrate in PEI solution. Hereby, a thin layer of PEI was formed in a first step. After extensive rinsing in water to remove loosely bound PEI molecules, AuNP were adsorbed from solution. Repeating these steps two or three times resulted in formation of samples 2X and 3X, respectively, according to Table I. These layers are characterised in this section.

Layers of type 1X (single adsorption cycle) were red coloured due to the absorption of plasmon waves and had an absorbance of 0.11 at a maximum absorption wavelength of 525 nm as displayed in the spectrum of Figure 3. The difference of the absorption maximum to that of AuNP in solution (520 nm) points to a different dielectric environment of the AuNP in the layer.²⁵ PEI had a higher dielectric permittivity (about 2.1) than water (1.77). Probably, they were at least partly embedded in PEI. Thus, the spectrum revealed that the layer consists mainly of single particles without plasmon interactions between them, as illustrated in Figure 4.²⁶

The layer of sample 2X was blue coloured. The absorption maximum was at a wavelength of 622 nm. This points to the formation of aggregates, in which particles were densely packed with small distances between them, so that their plasmon waves interact. Because of the different curve shape, no quantitative estimations of the absorbed amount based on the absorbance were made.

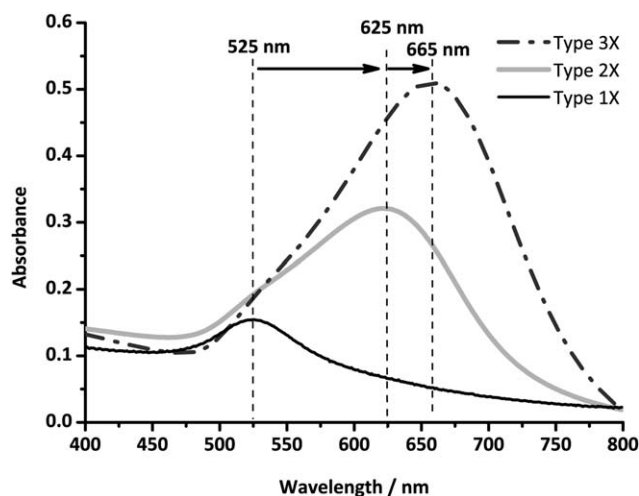


Figure 3. Optical spectrum of AuNP-PEI layers of type 1X (one adsorption cycle), 2X (two adsorption cycles), and 3X (three adsorption cycles) on glass slide.

The spectrum of samples of type 3X exhibited a stronger absorption and a larger shift than that of samples of type 2X. This suggests that the amount of AuNP aggregates in the layer was even higher. Nevertheless, the layer was still transparent. XPS studies confirmed the findings that the repetition of the coating process increased the number of AuNP on the substrate surface (see supporting information).

The SEM picture and the corresponding AFM picture of a typical sample of type 1X in Figure 5 showed mainly single AuNP on the substrate surface. Very few aggregates had formed during adsorption. This conclusion agrees with that of the spectroscopic investigations. All particles had nearly the same size. They were randomly distributed over the surface. The degree of area coverage was about 40%. Moreover, height analysis of AFM images revealed that the average height of the particles over the surrounding level was about 25 nm, as shown in Supporting Information Figure S2. This coincided with the particle diameter from DLS measurements and suggested that the AuNP were adsorbed on top of the PEI layer rather than integrated within PEI.

Sample 2X showed some single particles in the SEM image as well as in the AFM image. However, the amount of aggregates prevailed, as already concluded from the spectroscopic investigations. The amount of aggregates was even higher in the samples

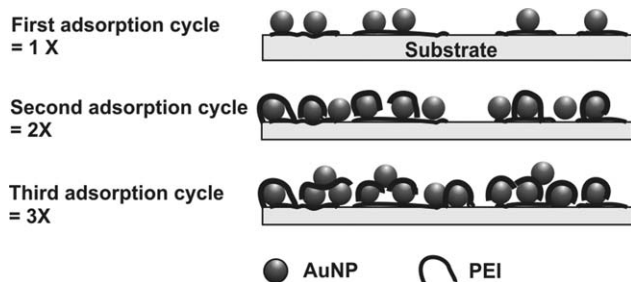


Figure 4. Schematic sample surface of Type 1X after first, type 2X after second and type 3X after third adsorption cycle (PEI and AuNP).

3X according to the SEM image. Almost no single particles were visible. The aggregates are larger than those in samples 2X, and they were frequently connected with each other. The degree of coverage was about 70%. The AFM height contrast image clearly shows aggregates, which seems to be partly in contact. The average height in AFM images was about 25 nm and agreed with that of 1X samples. Consequently, the AuNP were assembled within one layer rather than in a multilayer structure as described in literature.¹⁶ The degree of area coverage in these layers increased with the number of adsorption steps. The reason for that is probably found in the electrostatic adsorption process: Because the AuNP exhibited a negative surface charge in water (see Figure 2), the PEI adsorption in the second and third cycles took place preferentially on the surface of the AuNP. The following AuNP adsorption, again, took place preferentially on those areas, which were covered with PEI, thus in the vicinity of an already adsorbed AuNP. As a result, AuNP are adsorbed on the substrate surface preferentially chain-like.

Transfer of AuNP-PEI Layers to PC Surface using Injection Molding

The substrates, prepared and covered with the appropriate layers according to the procedures described above, were mounted in the mold of an injection molding machine. PC melt was injected into the mold to transfer the layer to the melt surface. After solidification, the part was ejected and the substrate was separated from the PC plate formed. As a result, the typical colour of the AuNP-PEI layer disappeared from the substrate. The PC plate surface was now coloured red or blue, similar to the substrate surface before the procedure. The AuNP-PEI layers on PC were resistant against rinsing and slight mechanical strain. This pointed to a successful transfer and permanent immobilisation on the PC surface. The contact angles against water were between 35 and 40 degrees, depending on sample preparation. Thus, the surfaces are much more hydrophilic than that of plain PC (97 degrees).

We investigated the structure of the AuNP layer on the PC surface and the influence of the molding process on it. To recall, PEI is a soft and fluid material and formed a layer on the substrate surface. The AuNP were embedded in this layer. During molding, it was faced to a melt flow in a certain direction. The SEM image of sample 1X in Figure 6 shows a random distribution of the AuNP over the surface, similar to that on the substrate surface before the transfer. The micrographs did not reproduce any flow direction. This pointed to a strong fixation of the nanoparticles on the substrate. The melt typically moves in a fountain flow, where the melt approaches the mold surface perpendicularly.²⁷ Consequently, the fountain flow must be rather perfectly realised in our experiments, also in the range of nanometres at the mold surface. However, capillary forces between melt and particles could occur.¹⁷ A detailed analysis of the melt flow over nanoparticulate objects may be interesting.

Sample 2X exhibited a higher degree of coverage in the SEM image than found for samples 1X. The particles here formed mostly two-dimensional aggregates. The image of sample 3X revealed a high degree of coverage with only few unoccupied areas. It suggested that many particles are in contact with their

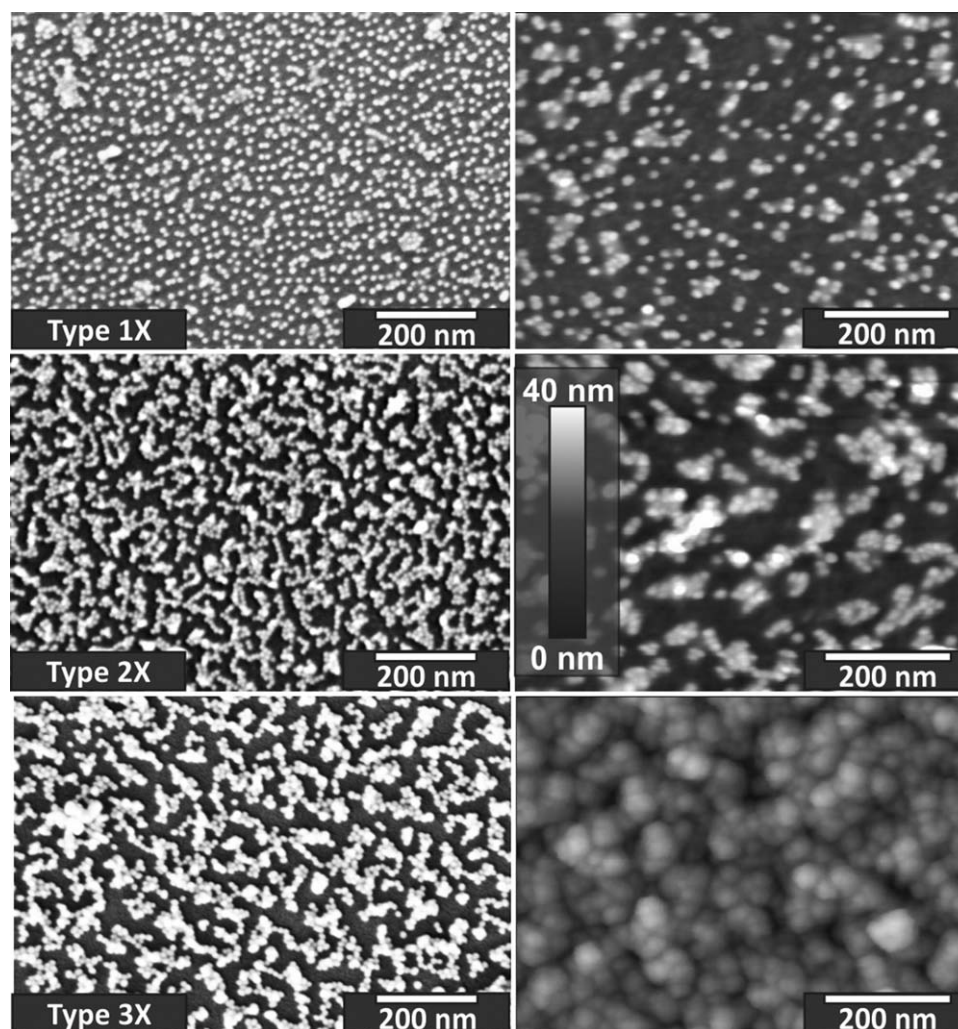


Figure 5. SEM images (left) of glass surfaces with AuNP-PEI layers of type 1X, 2X and 3X, prepared by electrostatic adsorption. The maximum height in all AFM images (right) is 40 nm, mainly caused by AuNP agglomerates on the substrate.

neighbours and, thus, formed one large two-dimensional aggregate. Thus, the SEM investigations revealed no change of the lateral structure of the assemblies during transfer from the substrate surface to the thermoplastic part surface. The average heights of the particles on the PC surface taken from the AFM profiles were about 10 nm for samples of type 1X, 2X, and 3X (see Supporting Information Figure S3). This was about half the height of the layer adsorbed on the substrate. Hence, we presume partly embedding of the particles.

Thin cuts of each sample type were made by focused ion beam and investigated by TEM. The TEM micrograph of sample 1X in Figure 7 clearly shows single particles as dark grey objects. They were arranged in a loosely organised monolayer as already suggested by SEM images. Some AuNP seemed to be in contact, but this may be an artefact due to cutting during sample preparation. The thickness of the cut was larger than the AuNP diameter, and the cut surface might not be exactly perpendicular to the electron beam. Darker objects indicated successive arrangements of two or more particles. The image revealed surprisingly, that the AuNP were embedded in a rather defined arrangement during injection

molding in the outermost surface layer of a PC part, like in one straight line. Some of the particles may be covered by PC, but most were only partly embedded.

The particles of sample 2X were also well ordered on the surface. However, the density of particles in the plane was higher. Moreover, more dark particles were visible, suggesting that some particles were arranged behind the particles seen in the first row. The particles in sample 3X were even denser packed. The micrograph suggested formation of three-dimensional aggregates, but this might be again an artefact due to cutting during the sample preparation. Nevertheless, it is clearly visible that the AuNP were arranged in a straight line with deviations less than a particle diameter, as indicated by the white line in the micrograph.

Energy filtered transmission electron microscopy (EFTEM) investigations (see Supporting Information Figure S4) were carried out to detect the distribution of nitrogen, stemmed from PEI, in these arrangements. PEI was detected in the EFTEM micrographs mainly within the AuNP-PEI layers and between the AuNP. PEI was not found on the surface of the AuNP,

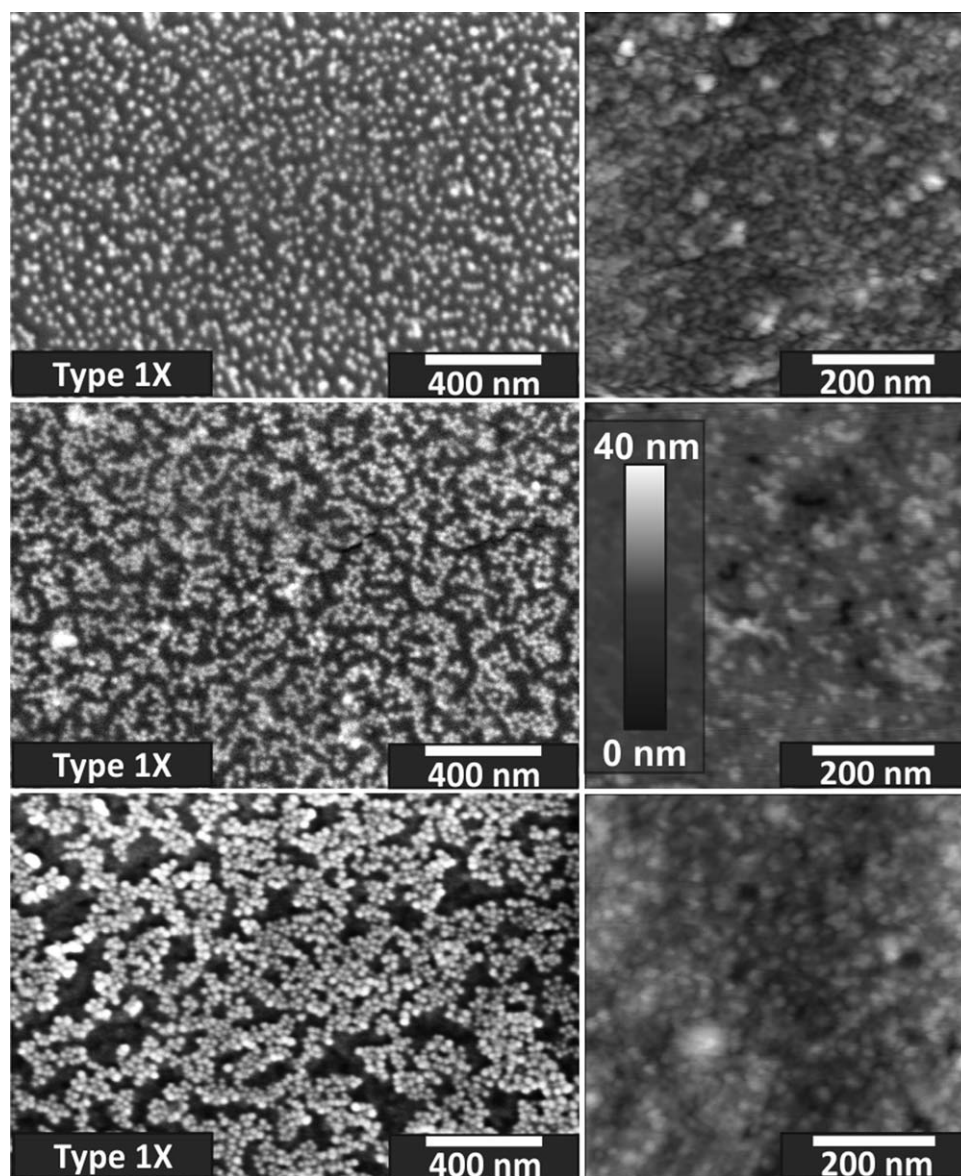


Figure 6. SEM images (left) of PC surfaces with AuNP-PEI layers, prepared from substrates of Type 1X, 2X, and 3X. The maximum height in all AFM images (right) was 40 nm, mainly caused by curvature of the thermoplastic part surface.

probably because of a high quantification limit of the method. However, XPS studies clearly showed the presence of PEI on the PC surface, which was decorated with AuNP. The deconvolution of the N 1s and Au 4f high-resolution XPS spectra (see Supporting Information Figures S5 and S6) indicated coordinative bonds between the nitrogen atoms of the amino groups and the gold surface. The strong interactions were driven by an electron transfer from the nitrogen's non-bonded electron pair to the Au 6s orbitals of the gold atoms and the resulting electron back-donation from gold to the nitrogen atoms. These findings clarified that the bonding of PEI and AuNP was not only supported by electrostatic interactions.

The structural investigations revealed that the AuNP were arranged in a thin layer on the surface of PC with a thickness close to the AuNP diameter (about 20 nm in average). The particle density increased with the number of adsorption steps of

AuNP. Single particles were formed at beginning, and two-dimensional aggregates, where the particles are connected with each other, were formed at high density. This was concluded from SEM and TEM images as well as from optical absorption spectra. The localisation within one layer was rather strong, so that a high stability of the layer on the substrate against mechanical shift due to flowing melt is assumed. The AuNP were partly embedded on the PC surface. Because the AuNP were adsorbed on a PEI layer on the substrate in advance, and a layer inversion took place during transfer to the thermoplastic part surface, the AuNP could also be covered by PEI. If the surface properties of gold should be exploited in this assembly, then the gold surface must be accessible for small molecules from the surrounding medium. A typical application of gold in microfluidics is catalysis. Therefore, we investigated the catalytic activity.

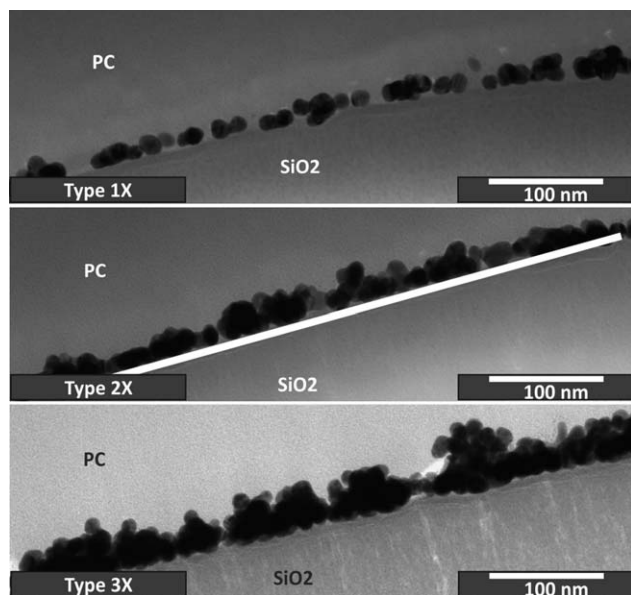


Figure 7. TEM micrographs of thin sections perpendicular to the surface. The white line is parallel to the surface. The layers were transferred from a substrate, which was coated with AuNP/PEI layers of Type 1X, 2X, and 3X. Thin sections with a thickness of 50 nm were prepared by focused ion beam lamellas cutting. To protect the samples during cutting, they were coated with a thin carbon layer and a silicon dioxide layer.

Chemical Activity of AuNP-PEI Layers on PC Surface

In the following experiments, the absorbance of MO solution in water mixed with NaBH_4 was measured in a glass cuvette over time at its maximum absorption wavelength at 463 nm.²¹ The absorbance was used as a measure for concentration of MO. No significant decrease of the absorbance was observed over several hours. No decrease was either detected, when glass slides or PC plates, only covered with PEI, were used. Then, AuNP-PEI coated glass slides or PC parts, respectively, were placed in a cuvette outside of the light pass. The absorbance decreased rapidly in the presence of glass slides coated with AuNP-PEI of type 1X, as shown in Figure 8. Obviously, MO was reduced by

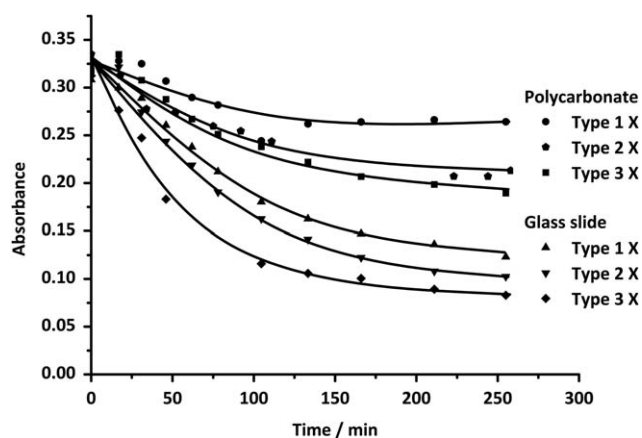


Figure 8. Absorbance of MO solutions during reaction with NaBH_4 in presence of AuNP-PEI layers adsorbed on glass slides and in presence of corresponding AuNP-PEI layers on PC, transferred by injection molding. The lines are added as a guide for the eyes.

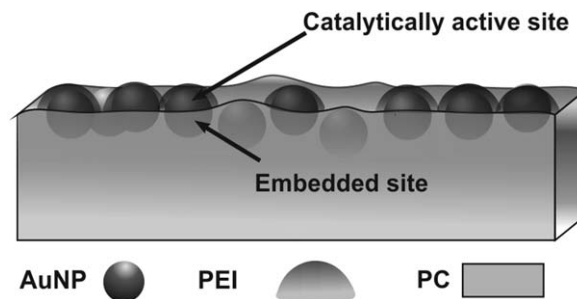


Figure 9. Model of the structure of the AuNP-PEI layer formed on molded PC.

borohydride, and the reaction was catalysed by gold. For this, a borohydride molecule and a MO molecule must be in contact with a AuNP. This demonstrates that the surface of AuNP adsorbed on glass is accessible for small molecules. The surfaces of the particles were oriented towards the solution due to the sample preparation. Samples produced with method 2X and 3X accelerate the reduction even more due to the higher degree of coverage. However, the high acceleration suggests that not only AuNP from the last adsorption step took part in the catalysis reaction, but also the AuNP adsorbed in previous steps, thus, the PEI layer between the particles did not prevent the diffusion of MO and of borohydride molecules and their attachment onto AuNP surfaces. The absorbance did not approach to zero due to the self-decomposition of borohydride at long times.

The same investigations of catalytic decomposition of MO were made with AuNP transferred to PC surface by molding. The decrease of the absorbance for the sample 1X with AuNP-PEI transferred to PC suggests that also the embedded AuNP were accessible for the small molecules and were catalytically active. A possible structure is proposed in Figure 9. The lower rate in comparison to sample 1X on glass could be a result of partly embedding of the AuNP in PC, which reduced the free surface area. Moreover, the number of AuNP per area might be smaller because the transfer ratio of AuNP from substrate to PC was smaller than unity on a micro scale. The reduction rate was much higher for samples 2X because of their higher degree of coverage. Samples of type 3X exhibited an even higher activity, but the increase was not proportional to the increase of degree of coverage. Probably, some parts of the particle surface were covered by other particles due to the high particle density on the surface.

CONCLUSIONS

Layer systems prepared by step-by-step electrostatic adsorption of AuNP and PEI on glass slides were formed and characterised. During the adsorption processes, the degree of area coverage was up to 70%. Due to the multiple step adsorptions, aggregates of AuNP were formed, as shown by optical absorption spectra, atomic force, and electron microscopy investigations. The aggregates typically consisted of particles arranged in a chain. At higher density, they arranged in a plane. Only rarely, three-dimensional aggregates were formed. The lateral structure on the substrate could be controlled by a multiple step adsorption process.

These layers were transferred from a substrate to PC by injection molding. By this, the particles were permanently immobilised on the PC part surface. The distribution on the PC part was similar to that on the substrate. Structure characterisation revealed that the AuNP were embedded within the outermost surface layer of the part. The embedding depth was smaller than the particle diameter. The catalytic reduction of MO was studied as model reaction. The catalytic activity suggested that parts of the surface area of the AuNP were indeed accessible for small molecules like MO and the borohydride anion.

The described method for immobilisation of AuNP on polymer part surfaces by molding presents an approach for the fabrication of active polymer surfaces. This may be advantageous for applications, where the effect of nanoparticles is desired only on the surface of a thermoplastic part. Excitation of plasmon waves in AuNP may be used to selectively generate heat at nanometre regions close to the surface of a thermoplastic part inducing chemical reactions. By use of this method, other types of nanoparticles could also be embedded. Applications may range from designing of antibacterial or scratch-resistant surfaces, the control of the surface properties like wettability, friction, up to catalytic reactions like solar energy conversion or in microfluidics.

ACKNOWLEDGMENTS

The support by the German Research Foundation under the project number HE4466/17-1 is greatly acknowledged. The authors wish to thank Mrs. Anja Caspari for DLS and electrokinetic measurements. We also thank Mr. Michael Göbel for the preparation of TEM lamellae. Bayer MaterialScience AG is acknowledged for providing the polycarbonate polymer.

REFERENCES

1. Bond, G. C.; Sermon, P. A.; Webb, G.; Buchanan, D. A.; Wells, P. B. *J. Chem. Soc. Chem. Commun.* **1973**, 444b.
2. Fenger, R.; Fertitta, E.; Kirmse, H.; Thunemann, A. F.; Rademann, K. *Phys. Chem. Chem. Phys.* **2012**, *14*, 9343.
3. Hashmi, A. S. K.; Hutchings, G. J. *Angew. Chem. Int. Ed.* **2006**, *45*, 7896.
4. Haruta, M. *Nature* **2005**, *437*, 1098.
5. Azad, U.; Ganesan, V.; Pal, M. *J. Nanopart. Res.* **2011**, *13*, 3951.
6. Chen, M.; Kang, H.; Gong, Y. *ACS Appl. Mater. Interfaces* **2015**, *7*, 21717.
7. Junejo, Y.; Sirajuddin, S.; Baykal, A.; Safdar, M.; Balouch, A. *Appl. Surf. Sci.* **2014**, *290*, 499.
8. Qi, Z.; Honma, I.; Ichihara, M.; Zhou, H. *Adv. Funct. Mater.* **2006**, *16*, 377.
9. Zhang, Z.; Liu, J.; Qi, Z. M.; Lu, D. F. *Mater. Sci. Eng. C* **2015**, *51*, 242.
10. Brust, M.; Bethell, D.; Kiely, C. J.; Schiffrin, D. J. *Langmuir* **1998**, *14*, 5425.
11. Zsigmondy-Göttingen, R. *Zeitschrift für Elektrochemie und angewandte physikalische Chemie* **1917**, *23*, 148.
12. Köth, A.; Koetz, J.; Appelhans, D.; Voit, B. *Colloid Polym. Sci.* **2008**, *286*, 1317.
13. Köth, A.; Tiersch, B.; Appelhans, D.; Gradzielski, M.; Cölfen, H.; Koetz, J. *J. Dispers. Sci. Technol.* **2011**, *33*, 52.
14. Zare, D.; Akbarzadeh, A.; Bararpour, N. *Int. J. Nanosci. Nanotechnol.* **2010**, *6*, 223.
15. Xu, M. M.; Yuan, Y. X.; Yao, J. L.; Han, S. Y.; Wang, M.; Gu, R. A. *J. Raman Spectrosc.* **2011**, *42*, 324.
16. Schmitt, J.; Decher, G.; Dressick, W. J.; Brandow, S. L.; Geer, R. E.; Shashidhar, R.; Calvert, J. M. *Adv. Mater.* **1997**, *9*, 61.
17. Deshmukh, R. D.; Composto, R. J. *Langmuir* **2007**, *23*, 13169.
18. Nagel, J.; Chunsod, P.; Zimmerer, C.; Simon, F.; Janke, A.; Heinrich, G. *Mater. Chem. Phys.* **2011**, *129*, 599.
19. Frens, G. *Kolloid-Z.u.Z. Polymere* **1972**, *250*, 736.
20. Kimling, J.; Maier, M.; Okenve, B.; Kotaidis, V.; Ballot, H.; Plech, A. *J. Phys. Chem. B* **2006**, *110*, 15700.
21. Li, W.; Li, J.; Qiang, W.; Xu, J.; Xu, D. *Analyst* **2013**, *138*, 760.
22. Rios-Corripio, M. A.; Garcia-Perez, B. E.; Jaramillo-Flores, M. E.; Gayou, V. L.; Rojas-Lopez, M. *J. Nanopart. Res.* **2013**, *15*, 1624.
23. Kelly, K. L.; Coronado, E.; Zhao, L. L.; Schatz, G. C. *J. Phys. Chem. B* **2002**, *107*, 668.
24. Schmitt, J.; Mächtle, P.; Eck, D.; Möhwald, H.; Helm, C. A. *Langmuir* **1999**, *15*, 3256.
25. Liu, X.; Atwater, M.; Wang, J.; Huo, Q. *Colloid. Surf. B: Bio-interfaces* **2007**, *58*, 3.
26. Sendroiu, I. E.; Mertens, S. F. L.; Schiffrin, D. J. *Phys. Chem. Chem. Phys.* **2006**, *8*, 1430.
27. Yoshii, M.; Kuramoto, H.; Kawana, T. *Polym. Eng. Sci* **1996**, *36*, 819.